Estimation of soil water content and evapotranspiration from irrigated cropland on the North China Plain

Jie Jiang[1], Yongqiang Zhang[2]*, Martin Wegehenkel[3], Qiang Yu[1], and **Jun Xia[1]**

[1] 1Institute of Geographic Sciences and Natural Resources Research, Chinese Academy of Sciences, No Jia 11., Datun Road, Anwai, Beijing 100101, China

[2] CSIRO–Land and Water, GPO Box 1666, Canberra ACT 2601, Australia

[3] Department of Landscape System Analysis, Centre of Agricultural Landscape and Land use Research (ZALF), Eberswalder Str. 84, 15374 Müncheberg, Germany

Abstract

For nearly 30 y, cropland on the North China Plain (NCP) has been irrigated primarily by pumping groundwater with no sustainable management strategy. This has caused a continuous decline of the water table. A sustainable groundwater management and irrigation strategy must be established in order to prevent further decline of the water table; to do this, one must quantify soil water content and daily rates of deep percolation and locate evapotranspiration from irrigated cropland. For that purpose, we developed a three-layer soil–water balance (SWB) model based on an approach described by *Kendy* et al. (2003). In this model, the unsaturated soil zone is divided into three layers: a surface active layer, a middle active soil layer, and a lowest passive soil layer. The middle and the lowest layers dynamically change with the development of crop rooting depth. A simple "tipping bucket" routine and an exponential equation are used to redistribute soil water in the three soil layers. The actual evapotranspiration estimated is partitioned into soil evaporation and crop transpiration using a dual crop coefficient reference approach. At first, the model was calibrated using data obtained from five deficiently irrigated field plots located at an experimental site in the NCP between 1998 and 2003. Then, the model was validated by comparing estimated soil water contents with measured ones at three other plots with nondeficient irrigation. The estimates of actual evapotranspiration were compared with those measured with a large-scale weighing lysimeter (3 m^2). The index of agreement (*IA*) for soil water contents varied between 0.62 and 0.80; the concordance correlation coefficient (*CCC*) and the root mean square error obtained from the same comparison were 0.34–0.65 and 0.043–0.074 $cm^3\,cm^{-3}$, respectively. The rates of 10 d mean evapotranspiration estimated by the model show a good fit to those measured by the large-scale lysimeter; this is indicated by *IA* = 0.94 and *CCC* = 0.88. Our results indicate that at the irrigated cropland on the plain, deep soil water–percolation rates are usually <200 mm y^{-1} under nondeficient-irrigation conditions.

Key words: soil water balance / soil water content / evapotranspiration / cropland / model / North China Plain

Accepted September 18, 2007

1 Introduction

The North China Plain (NCP), with an area of 3.5×10^5 km^2, is one of most important centers of agricultural production in China and home to >200 million people and to China's capital Beijing, which is located in its northern part. A lack of water limits crop production on the NCP (*Zhang* et al., 2004). Because of the monsoon, rainfall is spatially and temporally variable. Mean annual precipitation ranges between 400 and 600 mm y^{-1}, of which most falls from June to September. However, mean annual crop evapotranspiration (*ET*) under normal irrigation ranges between 800 and 900 mm y^{-1}, which exceeds annual precipitation (*Liu* et al., 2002). To maintain a high crop-grain yield, crops are irrigated by pumping groundwater. Because agricultural and industrial demand for groundwater has increased rapidly over the last two decades, the water table has dramatically declined in many areas of the plain (*Zhang* et al., 2001). For policy-makers to scientifically manage the limited water resources in this area, it is crucial to correctly quantify actual crop evapotranspiration (ET_a), soil water content, and groundwater recharge in irrigated cropland. In order to quantify these values, an appropriate, precise, physically based, and easy to use modeling approach is required.

Several approaches have been applied to estimate soil water balance (SWB) and ET_a so as to optimize irrigation procedures in the plain (*Li* et al., 2005; *Liu* et al., 1998; *Shang* et al., 2004; *Wang* et al., 2001; *Zhu* et al., 2005). These approaches are calibrated and validated across a wide range of water content and irrigation conditions, although long-term

* Correspondence: Dr. Y. Zhang; e-mail: yongqiang.zhang@csiro.au

soil–water content data are not available. Other studies do not consider deep water percolation in the soil–water balance equation (*Huang*, 2004; *Liu* et al., 1998). In order to estimate deep water percolation in unsaturated soil layers, a simple mechanistic ten-layer SWB model was developed and applied to irrigated cropland in the plain (*Kendy* et al., 2003). The data required for the model are readily obtainable; however, the model does not estimate ET_a rates well.

In this study, the main objectives were (1) to further simplify this mechanistic ten-layer SWB model, (2) to provide an approach to simulate soil water content at root depth, and (3) to estimate ET_a more correctly.

2 Material and methods

2.1 The variable three-layer soil–water balance model

We developed a variable three-layer SWB model that is simpler to operate, in which soil water percolation is based on the model of *Kendy* et al. (2003). In the new model, the soil reservoir is divided into three soil layers. The lower boundaries of a surface active layer and lowest passive layer are fixed, while that of a middle active layer is movable (Fig. 1). The surface active layer is fixed at a depth of 200 mm; the lowest passive layer is set at the maximum rooting depth, 2000 mm. The depth of the middle active layer dynamically varies according to rooting development (Fig. 1). If the actual crop rooting depth is shallower than the depth of the surface active layer, the middle layer disappears, if the crop root extension is deeper than the surface active layer, but does not reach the maximum rooting depth, the three layers are used, and when the roots attain the maximum rooting depth, the lowest soil layer disappears, and drainage from the lower boundary of the passive layer is regarded as deep percolation out of the soil reservoir.

Input data for the three-layer SWB model include daily meteorological data, crop data, initial soil-moisture data, and irrigation data. Meteorological data consist of daily maximum and minimum temperatures (°C), daily mean wind speed (m s^{-1}), daily sunshine duration (h), daily mean relative humidity, and daily precipitation rates (mm d^{-1}). Crop data consist of crop height (m) and rooting depth (mm). The parameters used in the model are listed with their meaning, symbol, unit, status, and method used to obtain them in Tab. 1. Outputs of the model include volumetric soil water content ($cm^3\,cm^{-3}$) in the three soil layers, soil water storage in the three soil layers (mm), soil evaporation (mm d^{-1}), crop transpiration (mm d^{-1}), and percolation from the bottom of the passive soil layer (mm d^{-1}).

2.1.2 Soil–water balance equations

The soil–water balance equations are based on the following assumptions. First, infiltration and evapotranspiration are treated as separate, sequential processes. Second, soil evaporation is limited to the upper active layer with a depth of 150 mm. Finally, transpiration is partitioned between the upper layer and the middle layer with an exponential function of layer thickness and rooting depth. Based on these assumptions, the soil–water balance equations in the three soil layers are:

$$\theta_{t,1}L_{t,1} = \theta_{t-1,1}L_{t,1} + I_t + P_t - RO_t - q_{t,1} - E_t - T_{t,1}, \quad (1)$$

$$\theta_{t,2}L_{t,2} = \theta_{t-1,2}L_{t-1,2} + q_{t,1} - q_{1,2} + \Delta R_t\,\theta_{t-1,3} - T_{t,2}, \quad (2)$$

$$\theta_{t,3}L_{t,3} = \theta_{t-1,3}L_{t,3} + q_{t,2} - q_{1,3}, \quad (3)$$

where t is the Julian date, 1, 2, and 3 are the soil layers from the surface to the maximum root depth (2000 mm), respectively, θ is the volumetric soil moisture ($cm^3\,cm^{-3}$), L is the thickness of the soil layer (mm), P is the precipitation (mm d^{-1}), I is the applied irrigation (mm d^{-1}), RO is the surface runoff (mm d^{-1}), E is the soil evaporation (mm d^{-1}), T is the crop transpiration (mm d^{-1}), q is the downflow flux (mm d^{-1}), and

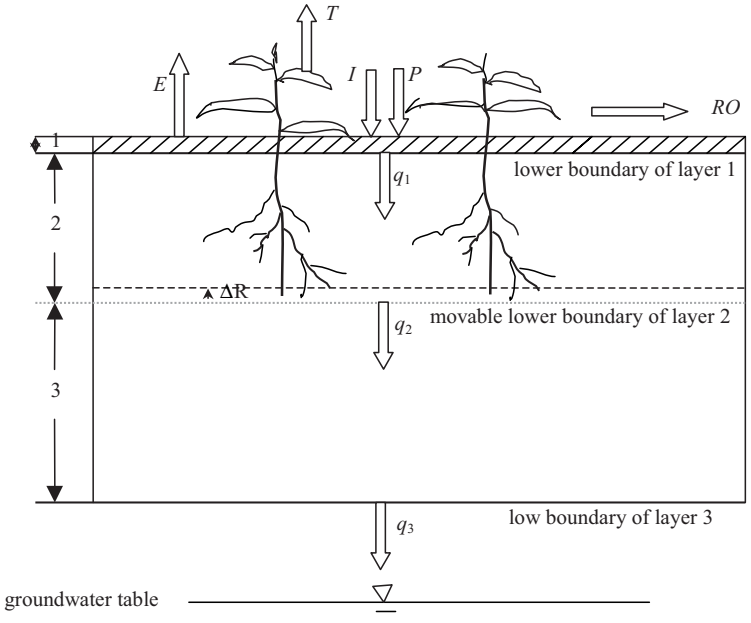

Figure 1: Sketch map of soil–water balance components in the three-layer soil–water balance model
* 1: surface active soil layer; 2: middle active soil layer; 3: bottom passive soil layer.
P = precipitation; I = irrigation; RO = surface runoff; T = crop transpiration; E = soil evaporation; ΔR = daily increase of rooting depth; q_1 = downflow from the bottom of the upper layer; q_2 = downflow from the bottom of the middle layer; q_3 = downflow from the bottom of the lowest layer.

ΔR, which equals $L_{t,2} - L_{t\text{-}1,2}$, is the rate of increase of crop rooting depth (mm d^{-1}).

2.1.3 Percolation submodel

The percolation submodel according to *Kendy* et al. (2003) estimates saturated and unsaturated water fluxes in the soil layers and assumes that gravity forces dominate over matrix forces in the soil. Modeled flux is therefore always downflow. First, precipitation or irrigation is added to the upper soil layer, which is filled to saturation. Water in excess of the layer's saturated soil moisture is distributed downward to the deeper layers in a "tipping bucket" fashion until either each layer is filled to saturation or all of the water has been distributed. Excess water that drains from the bottom of the passive soil layer is treated as groundwater recharge.

Assuming no incoming or outgoing water flux other than that produced by the unit gradient at the bottom of the layer, outflow from a layer can be expressed according to the conservation of mass as

$$L\frac{d\theta}{dt} = -K(\theta), \tag{4}$$

where K is the unsaturated hydraulic conductivity (mm d^{-1}). Equation 4 is solved using the following exponential relationship between K and soil water content (*Kendy* et al., 2003):

$$K(\theta) = K_{sat}\ exp\left(-\alpha\frac{\theta_s - \theta}{\theta_s - \theta_d}\right) \tag{5}$$

where K_{sat} is the saturated hydraulic conductivity, θ_s is the volumetric moisture content of the soil layer at saturation, θ_d is the soil water content at wilting point, and α is a site-specific parameter determined mainly from physical soil characteristics. For the same soil–water content conditions, the decrease of K is steeper for greater values of α (Fig. 2).

By substituting Eq. 4 into Eq. 5, separating variables, and integrating Eq. 5, we obtain the volumetric soil water content

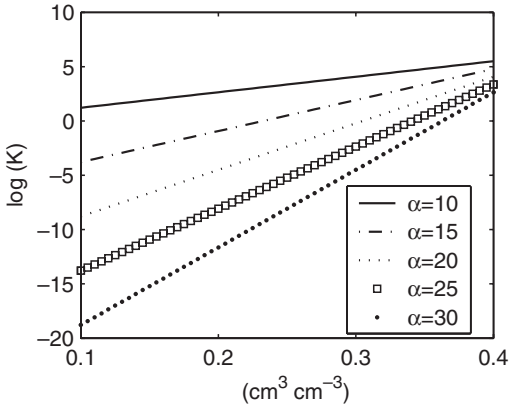

Figure 2: Logarithm of unsaturated hydraulic conductivity (K) *versus* volumetric soil water content (θ) using different empirical coefficients. The saturated hydraulic conductivity, K_s, is assumed to be 500 mm d^{-1}, saturated soil water content, θ_s, is assumed to be 0.45 cm^3 cm^{-3}; soil water content at wilting point, θ_d, is assumed to be 0.10 cm^3 cm^{-3}.

of a single layer after percolation (*Zhang* and *Wegehenkel*, 2006):

$$\theta_t = \theta_s - \frac{\theta_s - \theta_d}{\alpha}\ln\left[\frac{\alpha K_{sat}\Delta t}{L(\theta_s - \theta_d)} + \exp\left(\frac{\alpha(\theta_s - \theta_{t-\Delta t})}{\theta_s - \theta_d}\right)\right] \tag{6}$$

The flux into the deeper layer is the difference between θ_t and $\theta_{t-\Delta t}$.

2.1.4 Crop evapotranspiration submodel

The dual crop coefficient method developed by the Food and Agriculture Organization (FAO) of the United Nations was used to estimate crop ET_a (*Allen* et al., 1998). Estimating crop ET_a first requires obtaining a reference evapotranspiration (ET_0 [mm d^{-1}]), which is computed from weather data using the FAO-Penman-Monteith equation:

$$ET_0 = \frac{0.408\Delta(R_n - G) + \gamma\dfrac{900}{T_a + 273}u_2(e_s - e_a)}{\Delta + \gamma(1 + 0.34u_2)}, \tag{7}$$

where R_n is the net radiation at the crop surface (MJ m^{-2} d^{-1}), G is the soil heat flux density (MJ m^{-2} d^{-1}), T_a is the mean daily air temperature at 2 m height (°C), u_2 is the wind speed at 2 m height (m s^{-1}), e_s is the saturation vapor pressure (kPa), e_a is the actual vapor pressure (both in kPa) ($e_a = e_s \times RH$, RH is relative humidity), Δ is the slope of the vapor-pressure curve (kPa °C^{-1}), and γ is a psychrometric constant (kPa °C^{-1}), R_n is the difference between incoming net shortwave radiation (R_{ns}) and outgoing net long-wave radiation (R_{nl}). R_{ns} is estimated from surface solar radiation (R_s):

$$R_{ns} = (1 - \alpha_c)R_s, \tag{8}$$

where α_c is the albedo of the reference grassland, alfalfa. R_s is estimated as

$$R_s = \left(a_s + b_s\frac{S}{N}R_a\right), \tag{9}$$

where S is actual sunshine duration (h), N is maximum possible sunshine duration (h), S/N is relative sunshine duration (0–1), R_a is extraterrestrial radiation (MJ m^{-2} d^{-1}), and a_s and b_s are empirical coefficients. Soil heat flux densitx G is estimated with a simple calculation based on the idea that soil temperature follows air temperature. The detailed algorithms for R_n and G can be obtained from the FAO 56 ET method (*Allen* et al., 1998).

Actual evapotranspiration ET_a is determined by using ET_0 combined with the basal crop coefficient (K_{cb}), soil evaporation (K_e), and water stress (K_s):

$$ET_a = (K_{cb}K_s + K_e)ET_0. \tag{10}$$

According to Eq. 10, ET_a is partitioned into actual transpiration (T_{tot}) and soil evaporation (E):

$$T_{tot} = K_{cb}K_sET_0 \text{ and } E = K_eET_0. \tag{11}$$

The basal crop coefficient K_{cb} can be estimated from a given basal crop coefficient (K_{cb0}), meteorological data, and crop height (*Allen* et al., 1998):

$$K_{cb} = K_{cb0} + (0.04(u_2 - 2) - 0.004[(RH_{min} - 0.45)]) \times \left(\frac{h_c}{3}\right)^{0.3}, \quad (12)$$

where RH_{min} is the mean value for minimum relative humidity during the mid- or late-season growth stage for $0.2 \le RH_{min} \le 0.8$, and h_c is crop height (m). K_{cb0} varies for the initial, middle, and end crop phenological stages (Tab. 1) and is determined mainly by crop type, while K_{cb0} is influenced by local conditions, cultural practices, and crop variety as well. In most cases, local values for K_{cb0} do not deviate by >0.2 from the values recommended by the FAO 56 ET method (*Allen* et al., 1998).

The water-stress coefficient K_s, which varies from 0 to 1, is a dimensionless transpiration-reduction factor defined as follows:

$$K_s = \frac{TAW - D_r}{TAW - RAW} = \frac{TAW - D_r}{(1-p)TAW}, \quad (13)$$

where D_r is root-zone depletion (mm), *TAW* is the total available soil water in the root zone (mm) ($TAW = (\theta_f - \theta_d)L_r$; θ_f is

Table 1: Coefficient list in the variable three-layer soil–water balance model.

Symbol	Meaning	Unit	Used in	Way of obtaining	Value
K_{sat}	saturated hydraulic conductivity	mm d^{-1}	Eqs. 5 and 6	optimized	500 for layer1; 100 for layers 2 and 3
θ_s	saturated soil water content	cm^3 cm^{-3}	Eqs. 5 and 6	measurements (*Zhang* et al., 2002)	0.433 for layer 1; average at the depths of layers 2 and 3
θ_f	field capacity	cm^3 cm^{-3}	calculating TAW and TEW	measurements (*Zhang* et al., 2002)	0.364 for layer 1; average at the depths of layers 2 and 3
θ_d	soil water content at wilting point	cm^3 cm^{-3}	Eqs. 5 and 6	measurements (*Zhang* et al., 2002)	0.096 for layer 1; average at the depths of layers 2 and 3
α	exponential coefficient in hydraulic-conductivity equation	–	Eqs. 5 and 6	optimized	22 for layer 1; 15 for layers 2 and 3
α_c	albedo for the reference grassland	–	Eq. 8	*Allen* et al. (1998)	0.23
a_s, b_s	empirical coefficients in solar-radiation estimations	–	Eq. 9	optimized according to measurements	0.29 and 0.44
K_s	water-stress coefficient	–	Eqs. 10 and 11	defined in Eq. 13	variable
K_e	coefficient for soil evaporation	–	Eqs. 10 and 11	defined in Eq. 17	variable
K_{cb}	basal crop coefficient	–	Eq. 10	defined in Eq. 12	variable
K_{cb0}	given basal crop coefficient	–	Eq. 12	*Allen* et al. (1998)	0.15, 1.1, and 0.3 for initial, middle, and end stage, respectively
TAW	total available soil water in the root zone	mm	Eq. 13	$(\theta_f - \theta_d)\ L_r$	variable according to L_r
RAW	readily available soil water in the root zone	mm	Eq. 13	*pTAW*	variable
D_r	root-zone depletion	mm	Eq. 13	Eq. 85 (*Allen* et al., 1998)	variable
p	average fraction of TAW	–	Eq. 13	Eq. 14	variable
p_{give}	given threshold for p	–	Eq. 14	set constant	0.55
u_{tf}	transpiration-uptake fraction	–	Eq. 15	defined in Eq. 16	variable according to L_r
w_u	water use–distribution coefficient	–	Eq. 16	*Novak*,1987	3.64
K_r	dimensionless evaporation-reduction coefficient	–	Eq. 17	defined in Eq. 18	variable
K_{cmax}	maximum crop coefficient	–	Eq. 17	Eq. 72 (*Allen* et al., 1998)	1.05–1.30
f_{ew}	fraction of the soil that is both exposed and wetted	–	Eq. 17	Eq. 75 (*Allen* et al., 1998)	variable
TEW	maximum cumulative depth of soil evaporation	mm	Eq. 18	$(\theta_f - 0.5\theta_d)\ L_1$	47
REW	readily evaporable water in surface soil layer	mm	Eq. 18	set constant	15

the field capacity, L_r is rooting depth), *RAW* is the readily available soil water in the root zone (mm) (*RAW* = *pTAW*), and *p* is the average fraction of *TAW* that can be depleted from the root zone before moisture stress occurs. Root-zone depletion D_r is calculated from the soil–water balance equation in the root zone (see Eq. 85 in *Allen* et al. [1998]). Values of *p* are higher at low rates of ET_a under non-drought-stressed conditions than at high rates. An empirical approximation for adjusting *p* for ET_a rate is

$$p = p_{give} + 0.04\,(5 - ET_a), \tag{14}$$

where p_{give} is a given threshold used as a constant for *p*, limited to 0.1–0.8; p_{give} differs from one crop to another. For cereals such as barley, wheat, and maize, it has a value of 0.55 for $ET_a \approx 5.0$ mm d^{-1} (*Allen* et al., 1998). T_{tot} is partitioned into transpiration from the first layer (T_1) and that from the second layer (T_2) according to a transpiration uptake fraction (u^t_f):

$$T_1 = (1 - u^t_f)\,T_{tot} \text{ and } T_2 = u^t_f T_{tot}. \tag{15}$$

When $L_r < L_1$, u^t_f equals 0. When L_r is greater than L_1, u^t_f is estimated as follows, according to the assumed exponential distribution of crop roots:

$$u^t_f = \left(\frac{1}{1-\exp(-w_u)}\right)\left\{\exp\left[-w_u\left(\frac{L_l}{L_r}\right)\right] \times \left[1-\exp\left(-w_u\frac{L_r - L_l}{L_r}\right)\right]\right\}, \tag{16}$$

where w_u is a water-use distribution coefficient, which varies between 0 and 5 (*Kendy* et al., 2003); w_u is usually obtained from optimization or expert knowledge.

Soil evaporation K_e is calculated from

$$K_e = \min[K_r\,(K_{c\max} - K_{cb}),\ f_{ew}K_{c\max}], \tag{17}$$

where K_r is the dimensionless evaporation-reduction coefficient depending on the cumulative depth of water evaporated from the topsoil, f_{ew} is the fraction of soil that is both exposed and wetted, *i.e.*, the fraction of soil surface from which most evaporation occurs, and $K_{c\max}$ is the maximum value of the crop coefficient. K_r is calculated from

$$K_{r,t} = \begin{cases} 1 & D_e \le REW \\ \dfrac{TEW - D_{e,t-\Delta t}}{TEW - REW} & D_e > REW \end{cases}, \tag{18}$$

where $D_{e,\ t-\Delta t}$ is the cumulative depth of evaporation in mm from the surface layer at the end of day $t - \Delta t$, *TEW* is the maximum cumulative depth of evaporation from the soil surface layer, and *REW* is the readily evaporable water, *i.e.*, the maximum depth of water that can be evaporated from the topsoil layer without any restrictions (Tab. 1).

2.2 Experimental site and data

2.2.1 Experimental site

The field experiments for the model test were carried out at the Luancheng Agro-Ecosystem station (37°53′ N, 114°41′ E, and 50 m asl), located in Luancheng County in the NCP, where fertile topsoil and plenty of organic matter form a loam soil. The site belongs to the temperate semiarid monsoon climate, with a mean annual temperature of 12.2°C, a mean annual global radiation of 524 kJ cm^{-2}, and a mean annual precipitation of 481 mm. Most precipitation occurs from late June to September. The main crop system at the site involves doubly rotating winter wheat and summer maize. The growing season of winter wheat is from early October to mid-June, and that of maize is from early June to late September. Rainfall cannot meet the water consumption of winter wheat during the dry, windy spring season; as a result, five to six irrigations are needed to maintain high grain yield. Rainfall in a normal summer can usually satisfy the water consumption of maize, but a dry summer may require two to three irrigations. Large quantities of groundwater are pumped for irrigation, which caused the depth of the water table to drop to over 25 m beneath the soil surface in the experimental years.

2.2.2 Experimental data

The physical parameters of the soil profile, including saturated soil water content, field capacity, water content at the wilting point, and bulk density, were measured by sampling undisturbed soil columns at the seven soil depths 0–200, 200–350, 350–650, 650–950, 950–1450, 1450–1700, and 1700–1900 mm (*Zhang* et al., 2002). The parameter values of the 0–200 mm soil layer were used directly as the parameters for the first layer of the soil–water balance model, while those in lower soil layers were averaged to calculate corresponding parameters for the second and third layers of the model.

The daily meteorological data (including maximum temperature, minimum temperature, wind speed, relative humidity, and sunshine hours) were measured by an automatic meteorological observation station where grassland was cropped and normally irrigated during the experimental period 1998 to 2003 (Changchun Meteorological Instrument Research Institute, China). Daily precipitation rates were measured by summing up hourly tipping-bucket measurements. The rooting depths of winter wheat and maize were reported by *Zhang* (1999) as a function of the number of days since planting.

The ET_a has been measured by a large-scale weighing lysimeter since 1995. The lysimeter was constructed by The Institute of Geographical Science and Natural Resources Research, a part of the Chinese Academy of Sciences. It is 3 m^2 in area and 2.5 m deep and contains approx. 14,000 kg of undisturbed soil. It can accurately measure daily actual *ET* with 0.02 mm precision. The lysimeter has four parts: the main body, the weighing system, the drainage system, and the data-collection system. It is described in detail by *Zhang* et al. (2002). In the data-collection system, a signal amplifier

detects changes of displacement and pressure. Because the numerical data collector malfunctioned, data from the signal amplifier were read manually at 8:00 a.m. and 8:00 p.m., and the difference of the observation results was used to estimate daily *ET* rates. The lysimeter, which was surrounded by cropland, was situated approx. 20 m away from experimental field plots. Double-cropped winter wheat and summer maize, the same as on the adjacent field plots, were planted at the lysimeter, and irrigation for the lysimeter was the same as for the field plots with nondeficient-irrigation application. This means that the soil water content at the rooting depth was >80% field capacity.

The 16 field plots, each with an area of 50 m^2, were used for agricultural water-management experimentation since 1998 (*Zhang* et al., 2004). Each site was well irrigated prior to the model-calibration period. Five different irrigation schedules were applied for winter wheat and two were applied for maize (Tab. 2). The five plots 1, 2, 3, 4, and 7 were randomly irrigated with treatments from A to E during 1998 to 2003; these were used for model calibration. Plots 5, 6, and 8 were selected for model validation. Among them, plot 8 was irrigated with treatment A during the whole experimental period; plots 5 and 6 were irrigated with treatment E in the spring of 2002, but with treatment A all other times. Each plot was equipped with a neutron-probe access tube on October 1, 1998. Neutron probes (Institute of Hydrology, UK) were used to measure soil water content approximately every 5 days at 9–10 depth intervals between 0 and 180 cm depth for the time period 1998–2003. Measurements of the soil compartment 180–200 cm were also occasionally carried out. The neutron-probe measurements were calibrated by gravimetric soil-water measurements at 20 cm intervals at depths of 0–140 cm. The calibration equation at depths of 140–200 cm was assumed identical to that at depths 120–140 cm. Gravimetric samples for the soil depth 0–20 cm were taken simultaneously to calibrate neutron-probe measurements.

Net radiation above the cropland was measured in 1999 with a Q7–1 type net radiometer (Campbell Scientific, Logan, UT) with hemispherical polyethylene domes at Luancheng Station (*Zhang* et al., 2002). Readings were taken every 10 s, averaged over 20 min intervals, and logged with a data logger (Model CR10X, Campbell Scientific, Logan, UT).

Table 2: Irrigation treatments for winter wheat and maize at Luanchen station (1998–2003).

Crop	Treatment	Growth stage and irrigation treatment (θ/θ_f) [a]				
		winter dormancy	spring green up	stem extension	heading	grain filling
Winter wheat	A	1.0 [a]	–[b]	0.8	0.8	0.8
	B	1.0	0.8	–	0.8	0.8
	C	1.0	0.8	0.8	0.8	–
	D	1.0	1.0	1.0	1.0	1.0
	E	1.0	–	–	–	–
Maize	D	–	–	1.0	1.0	1.0
	E	–	–	–	–	–

[a] θ is average soil water content of crop root depth; θ_f is average field capacity of crop root depth. 1.0 or 0.8 means the ratio of θ *to* θ_f.
[b] "–" shows that no irrigation is applied.

2.3 Model calibration

Parameters K_{sat} and α were optimized with a nonlinear least-square Gauss-Newton method. The cost function was the lowest root mean square error between measured and estimated soil water content. The model ran for the first 2 years (1998–1999) to warm up. It was then calibrated using the measured soil water content of each fifth day and the simulated one at the same time from 2000 to 2003. Five calibrated plots 1, 2, 3, 4, and 7 were selected to optimize the parameters K_{sat} and α. We assume that K_{sat} and α in the middle and lowest passive layers are identical due to the dynamic change of thickness of these two layers. Therefore, K_{sat} and α were optimized in two layers. Averaged K_{sat} in each layer was obtained from the arithmetic average of the five optimized values for K_{sat}, as well as for averaged α. The average K_{sat} and α were then used for simulations in plots 5, 6, and 8.

2.4 Validation criteria of diagnostic variables

Model estimates were evaluated with four different approaches: the difference between observed and estimated means (*MAD*), the index of agreement (*IA*) (*Willmott*, 1981, 1984), the concordance correlation coefficient (*CCC*) (*Lin* et al., 2002; *Lin*, 1989), and the root mean square error (RMSE), as follows:

$$MAD = \mu_1 - \mu_2, \tag{19}$$

$$\mathrm{RMSE} = \sqrt{\frac{\sum_{i=1}^{N} (Y_1 - Y_2)^2}{N-1}}, \tag{20}$$

$$IA = 1 - \frac{\sum_{i=1}^{N} (Y_1 - Y_2)^2}{\sum_{i=1}^{N} [|Y_1 - \mu_2| + |Y_2 - \mu_2|]^2}, \tag{21}$$

$$CCC = \frac{2\sigma_{1,2}}{\sigma_1^2 + \sigma_2^2 + (\mu_1 - \mu_2)^2}, \tag{22}$$

where Y_1 and Y_2 are the estimated and measured values, respectively; μ_1 and μ_2 are the means of estimated and measured values, respectively; N is the sample number, and $\sigma_{1,2}$, $\sigma^2{}_1$, and $\sigma^2{}_2$ are vectors in the covariance matrix of estimated and measured pairs. The *IA* results in a range between 0 and 1; the closer it is to 1, the better the fit between observed and estimated values. The *CCC*, which evaluates the degree to which pairs fall on the 45° line through the origin, is scaled to between –1 and 1.

3 Results

3.1 Optimization of parameters

For the upper layer, the optimized K_{sat} varied between 479 and 528 mm d^{-1} in the five calibration plots 1, 2, 3, 4, and 7, with an average K_{sat} of 502 mm d^{-1} and a K_{sat} standard deviation of 17.2 mm d^{-1}. For the middle layer as well as in the lowest layer, the optimized K_{sat} changed from 105 to 119 mm d^{-1}, with an average value of 113.4 mm d^{-1} and a standard deviation of 6.3 mm d^{-1}. For an undisturbed loam soil on the NCP, K_{sat} was measured approx. 2,300 mm d^{-1} for the soil layer from 0 to 250 mm deep and 17–500 mm d^{-1} for deeper soil layers (*Deng* et al., 2002). The optimized K_{sat} in the upper active layer was evidently lower than the measured one because the surface soil layer at our site was highly disturbed due to continuous cropping (*Deng* et al., 2002).

The optimized α for the surface layer varied between 15.0 and 21, with a small standard deviation of 2.7 and an average value of 18.5; that for the other two layers varied between 14 and 19, with an average value of 15.5 and a smaller standard deviation of 2.0. The α optimized for the surface layer was slightly higher than that by the trial-and-error adjustment calibration, for which α was estimated at 13–16 in ten soil layers from 0 to 2000 mm depth (*Kendy* et al., 2003). The optimized α for the other two layers, however, was almost same as that in *Kendy* et al. (2003).

The calibrated model simulated soil water content in the lower two layers better than in the upper layer. In the upper layer, the cost function RMSE varied between 0.07 and 0.09, with an average of 0.082 and a standard deviation of 0.006. In the lower layers, RMSE changed from 0.04 to 0.07, with an average of 0.057 and a standard deviation of 0.007.

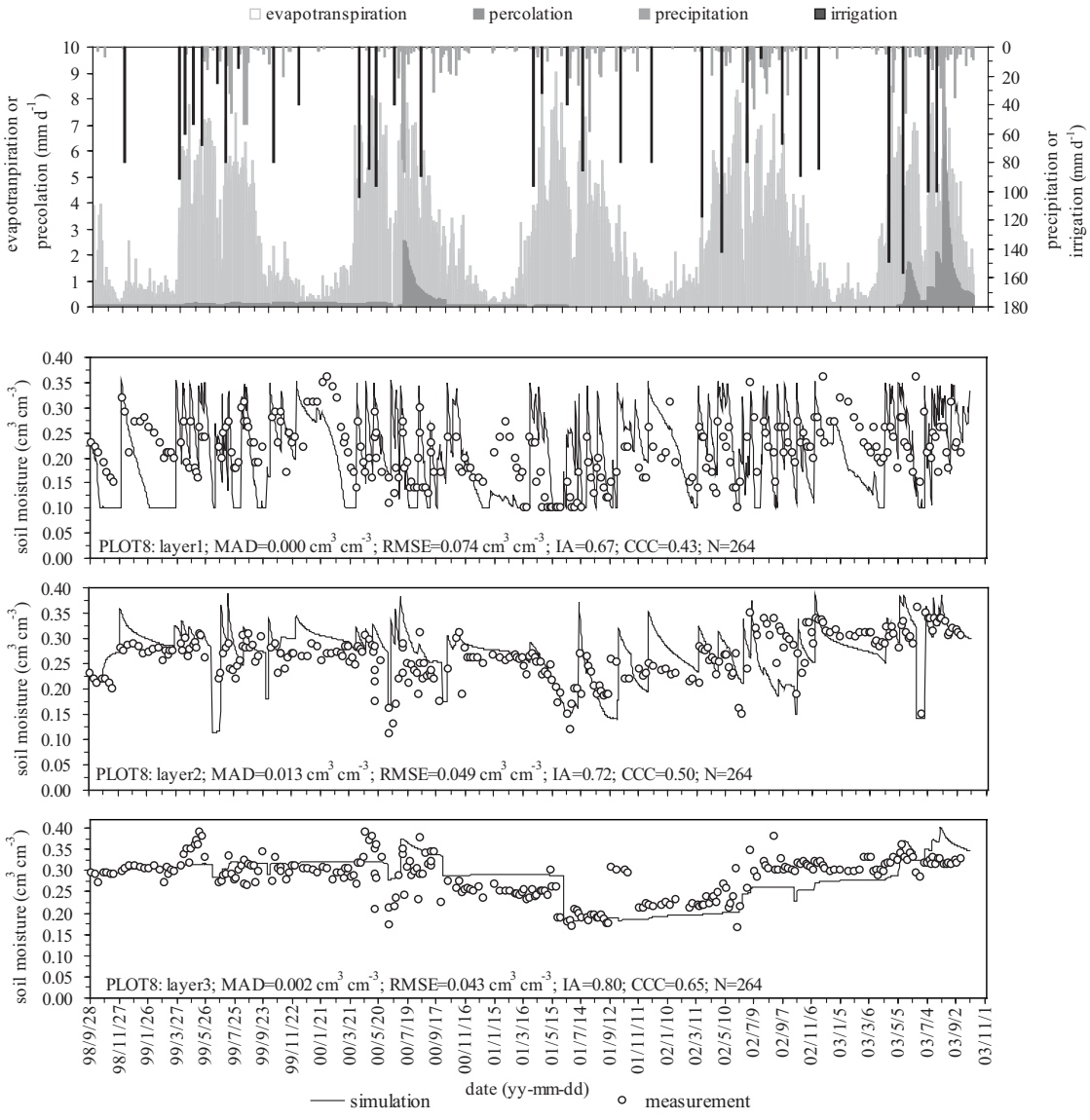

Figure 3: Seasonal dynamics of measured and estimated soil water content (cm^3 cm^{-3}) at the three soil layers (surface active layer, middle active layer, and lowest passive layer), and evapotranspiration, deep soil-water percolation, precipitation, and irrigation at plot 8 with nondeficient irrigation.

Table 3: Estimated soil–water balance components at three irrigated plots from 1998 to 2003. P = Precipitation; I = irrigation; T_{tot} = crop transpiration; E = soil evaporation; ET_a = actual evapotranspiration; q_3 = soil-water percolation beneath the maximum rooting depth; S = soil-moisture change.

plot	Year	P	I	ET_0	T_{tot}	E	ET_a	q_3	ΔS
No.5	1988-10-01–1999-09-30	347	487	938	644	159	803	89	–58
	1999-10-01–2000-09-30	402	504	935	684	146	830	95	–19
	2000-10-01–2001-09-30	344	436	937	661	178	838	7	–66
	2001-10-01–2002-09-30	399	160	949	563	170	732	1	–175
	2002-10-01–2003-09-30	476	393	877	579	172	751	0	118
No.6	1998-10-01–1999-09-30	347	487	938	644	163	807	64	–37
	1999-10-01–2000-09-30	402	553	935	684	146	830	136	–11
	2000-10-01–2001-09-30	344	486	937	666	177	843	10	–23
	2001-10-01–2002-09-30	399	160	949	597	162	760	6	–206
	2002-10-01–2003-09-30	476	468	877	589	172	761	1	182
No.8	1998-10-01–1999-09-30	347	473	938	644	156	800	31	–11
	1999-10-01–2000-09-30	402	534	935	684	146	830	101	5
	2000-10-01–2001-09-30	344	334	937	662	171	833	9	–164
	2001-10-01–2002-09-30	399	495	949	656	187	843	1	50
	2002-10-01–2003-09-30	476	680	877	590	172	761	181	213

3.2 Model validation: Prediction of soil water content

Figure 3 shows the seasonal variation of measured and simulated soil water content at plot 8. The simulated soil water content corresponded well with that measured, indicated by a RMSE between 0.043 and 0.074 $cm^3\,cm^{-3}$ and an *IA* varying between 0.67 and 0.80 in the three soil layers. Simulation quality increased continuously from the upper layer to the middle layer and to the lowest layer.

The simulation quality was further evaluated at plots 5 and 6 (Tab. 4). Comparisons of measured and simulated soil water content at the three plots indicated a MAD between –0.026 and 0.014 $cm^3\,cm^{-3}$, RMSE between 0.043 and 0.070 $cm^3\,cm^{-3}$, *IA* between 0.62 and 0.80, and *CCC* between 0.34 and 0.65. The middle layer was better simulated than was the upper layer when evaluated by MAD and RMSE but not by *IA* and *CCC*. The lowest layer was simulated best compared to the other two layers. The best simulation quality was found at plot 8.

Table 4: Validation-criteria analysis of soil water content at the three plots 5, 6, and 8. MAD and RMSE are in the same unit of $cm^3\,cm^{-3}$; n is sample number.

Layer	Plot	MAD	RMSE	*IA*	*CCC*	n
1	5	–0.026	0.070	0.73	0.53	258
1	6	–0.026	0.074	0.70	0.49	258
1	8	0.000	0.074	0.67	0.43	258
2	5	0.000	0.056	0.62	0.34	258
2	6	0.014	0.051	0.66	0.41	258
2	8	0.013	0.049	0.72	0.50	258
3	5	–0.01	0.054	0.72	0.53	264
3	6	0.003	0.046	0.75	0.56	264
3	8	0.002	0.043	0.80	0.65	264

3.3 Model validation: Prediction of evapotranspiration

The seasonal variation of estimated ET_a for the validation plots 5, 6, and 8 agreed well with the ET_a measured by the large-scale lysimeter during 1998–2003 (Fig. 4). Estimated and measured ET_a both showed two peaks in the winter wheat season and the maize season, respectively. Measured and estimated minimum ET_a both appeared during winter dormancy in the winter wheat season. The quality of the estimated ET_a was analyzed by comparing mean measured and estimated ET_a rates over 10 d (Fig. 5). The values of *IA* = 0.94 and *CCC* = 0.88 suggested a good estimate of ET_a. A MAD of –0.34 mm d^{-1}, however, shows that estimated ET_a tended to be lower than measured rates (Fig. 5).

3.4 Annual outputs of the model

The annual rates of the estimated water-balance components for the three irrigated plots in the period 1998–2003 are summarized in Tab. 3. One year in Tab. 3 is defined from October 1 to September 30 the following year, because in the research area, winter wheat is sown in early October and harvested in mid-June and summer maize is sown in mid-June and harvested in late September. The water surplus due to irrigation and precipitation is mainly transpirated by crops and evaporated from soil. At irrigated plots with nondeficient irrigation, estimated annual rates of ET_a were within 800–850 mm y^{-1} during 1998–2002. In the period 2002–2003, the annual rates of ET_a for all the plots were only

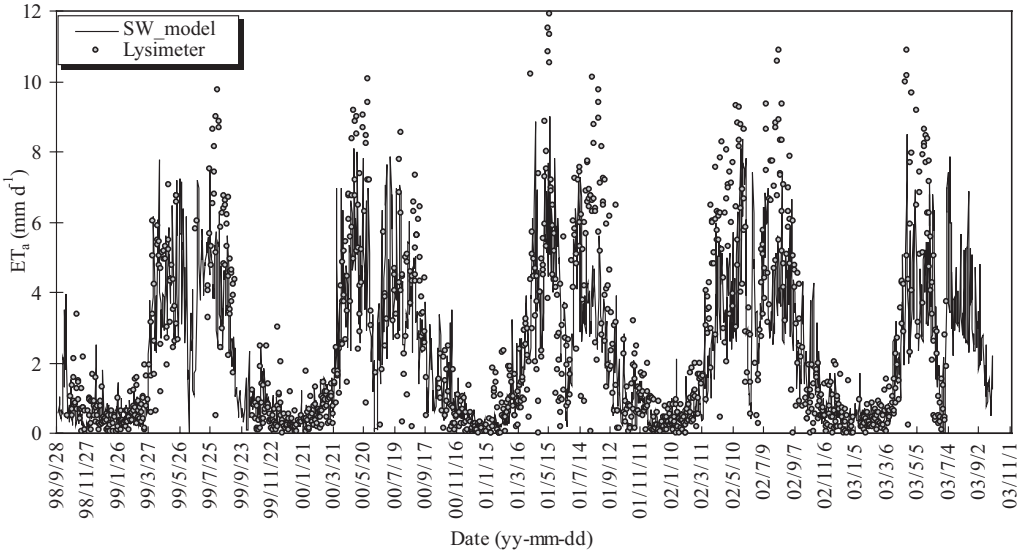

Figure 4: Seasonal change of lysimeter-measured evapotranspiration (ET_a) and simulated ET_a at plot 8 in 1998–2003.

approx. 750–760 mm y^{-1} because calculated annual rates of ET_0 in 2002–2003 were smaller than those in other years. In 2000–2001 and 2001–2002, only very low deep-percolation rates (<11 mm y^{-1}) were estimated at all plots. In 2002–2003 at plot 8, the annual rate of deep percolation was estimated at approx. 181 mm y^{-1} due to a high irrigation of 680 mm y^{-1} that was observed (Tab. 3). In contrast, in 2002–2003, very low deep-percolation rates were estimated at plots 5 and 6 due to low irrigation of 160 mm y^{-1} applied at the two plots in the previous year (Tab. 3). This indicates that low deep-percolation rates can occur with low rainfall and irrigation not only in the same year, but that it can also continue into the following year.

4 Discussion

4.1 Evaluation of estimated soil water content

The estimation of soil water content resulted in a RMSE varying from 0.043 to 0.074 cm^3 cm^{-3} for the three soil layers. Our result can be compared with estimation results by different agro-ecosystem models in which RMSE calculated by comparing estimated with observed volumetric soil water content was within 0.02 and 0.126 cm^3 cm^{-3} (*Diekkrüger* et al., 1995). In a similar study, a model for calculating field-scale water flow was validated, using TDR measurements (*Jacques* et al., 2002). Here, the RMSE for estimated and measured soil water content was between 0.038 and 0.125 cm^3 cm^{-3} (*Jacques* et al., 2002). In another study, two procedures in a SWB model were used to estimate soil water content (*Wegehenkel*, 2005). The *IA* and RMSE between the estimated and TDR-measured soil water content were 0.26–0.78 and 0.028–0.130 cm^3 cm^{-3}, respectively (*Wegehenkel*, 2005). The RMSE comparison between this and other results suggests that the variable three-layer model simulates soil water content well, especially for deep soil layers.

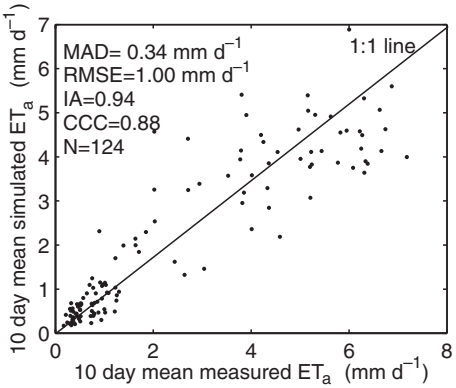

Figure 5: Comparison between lysimeter-measured evapotranspiration (ET_a) and simulated ET_a at plot 8.

In the surface soil layer, the estimated winter soil water content was lower than that measured. One possible reason is that we disregarded the capillary rise of water from the second layer, which may be significant when the topsoil becomes dry owing to a lack of water input (Fig. 3). Overestimating unsaturated hydraulic conductivity can also contribute to the underestimation of soil water content, because very low soil temperature in winter can reduce unsaturated hydraulic conductivity (*Giakoumakis* and *Tsakiris*, 1991; *Liu* et al., 2000). Snowfall in the model is considered directly as equivalent rainfall, and a snowmelt process is not included; as a result, soil evaporation is overestimated under snow-cover conditions. However, in the period from 1998 to 2003, snowfall only accounted for 1.5% of total precipitation, although snowfall frequency was approx. 10.5% of precipitation events. The impact of snowfall on surface water balance should therefore be very small.

4.2 Comparison between the current and previous model

The current SWB model uses the same percolation function as the previous one (*Kendy* et al., 2003) to redistribute soil

water content. There are three main improvements in the current model. The first is that soil layers were simplified from the former ten layers to the current three layers, in which the depths of the second and third layers change with the development of rooting depth; the second is that the dual K_c-ET_0 approach in the current model was used to quantify ET_a instead of the simple pan-evaporation method used in the former; and the third improvement is that the calibration method for α and K_s (the trial-and-error adjustment) in the former model was replaced by the nonlinear least-square Gauss-Newton method in the current model.

Compared to the former model (*Kendy* et al., 2003), the current model can much better estimate ET_0 and ET_a. In the former SWB model, ET_0 was estimated by measuring class A pan evaporation multiplied by a conversion coefficient of 0.7. However, this conversion coefficient strongly depends on the upwind fetch and on local advection (*Rana* and *Katerji*, 2000). In the current model, the FAO-Penman-Monteith method was used to quantify ET_0. The main energy-balance component R_n estimated from the FAO-Penman-Monteith method compared well with net radiometer-measured R_n, indicated by a RMSE of 2.09 MJ m^{-2} d^{-1}, an *IA* of 0.92, and a *CCC* of 0.85. Note that the FAO-Penman-Monteith method estimates R_n for grassland, while R_n is measured for cropland of winter wheat and maize.

Compared to the previous study (*Kendy* et al., 2003), this study improves simulation quality of daily ET_a. Between the measured and estimated daily ET_a, R^2 is approx. 0.74, compared with 0.58 in the previous study (*Kendy* et al., 2003). The scatter in Fig. 5 may be caused by random errors in both estimated and measured ET_a. Incorrect parameterization of crop coefficient and water-stress coefficient in the model can further contribute to the error. The well-known "oasis effect," mainly reflected by the lysimeter's metal and concrete frame, can cause higher ET_a rates in the lysimeter than in the surrounding cropland (*Zhang* et al., 2002).

Under nondeficient-irrigation conditions, the annual ET_a rate estimated by the previous approach (*Kendy* et al., 2003) was only prox. 680 mm y^{-1}, which was much lower than that measured with the large-scale–weighing lysimeter method carried out in the same research station (*Liu* et al., 2002). These measured ET_a rates ranged between 800 and 900 mm y^{-1}. Compared to the pan-evaporation-based ET_a method in the model of *Kendy* et al. (2003), the dual K_c-ET_0 approach in the new developed model estimated annual rates of ET_a between 730 and 843 mm at the three plots in 1998–2003. These values are only slightly lower than the lysimeter measurement, which is dubious due to the "oasis effect" discussed above.

The current model estimated soil water content in the first layer better than did the previous model, documented by the fact that the current model produced a RMSE varying between 0.070 and 0.074 cm^3 cm^{-3}, while the previous one produced 0.101 cm^3 cm^{-3} for the first layer (*Kendy* et al., 2003). We believe that this is due to the improved estimation of ET_a and the better calibration method in the current study.

4.3 Strong and weak points of the current SWB model

In our study, the "tipping bucket" method was applied to redistribute saturated soil water, and an exponential equation was used to estimate unsaturated hydraulic conductivity. The temporal dynamics of the deep-percolation rates estimated by our approach correspond more to natural conditions, compared to some other simple functional SWB models in which soil-water movement is not estimated (*Eitzinger* et al., 2003; *Huang*, 2004; *Jalota* and *Arora*, 2002). In comparison with similar SWB models (*e.g.*, model SAWAH; *Tenberge* et al., 1995), our modeling approach needs fewer coefficients in the soil–water flux equations. Compared to approaches using Richard's equation (*Maraux* et al., 1998; *Serrano*, 2004), the solution of the soil water–movement equations in our model needs less computing time because we avoid solving differential equations.

The depths of the middle active soil layer and the lowest passive soil layer in the current model dynamically change according to the development of crop rooting depth. In this case, the accuracy of estimated rooting depth directly influences the precision of estimates of soil moisture in the two layers. In our study, the development of crop rooting depth was estimated based on observation results in one year (*Zhang*, 1999). However, the real maximum rooting depth in different years might be different due to meteorological conditions and irrigation application, as discussed above. Therefore, the development of rooting depth might vary from year to year. As a result, the interface between the second and third layers might be poorly estimated.

To further simplify the model, we did not estimate snowmelt. Although winter temperatures can dip to –10°C at Luancheng station, precipitation during the winter is small. This simplification affects the accuracy of estimated soil water content in the surface soil layer in the winter (Fig. 3), but does not affect deeper soil layers.

5 Conclusions

The current model is useful for calculating the soil water balance in the northern China Plain, where the water table is declining continuously. The soil–water balance estimates (Tab. 3) show that double-cropped winter wheat and summer maize used approx. 750–850 mm y^{-1} soil water under nondeficient-irrigation treatment. Annual rainfall in the study years changed from 347 to 476 mm y^{-1}. To maintain this cropping system, at least 250 mm groundwater must be pumped each year. The model simulation suggests that rotating cropland results in the decline of the water table and that winter wheat must be replaced with low water–demanding economic crops.

The current SWB model is particularly suitable to areas with little topographic relief, relatively deep water tables, and insignificant snowmelt such as those in the northern China Plain. The model can provide an appropriate tool for the policy-makers in making sound decisions concerning soil–water balance issues in irrigated cropland when crop root depth is accurately estimated.

The estimation accuracy of the SWB model mainly depends on the following conditions: (1) physical parameters of soil profiles to quantify soil water redistribution in a saturated or unsaturated soil layer, (2) crop rooting depth determining the middle active soil layer and the lowest passive soil layer, and (3) the empirical parameter, for quantifying unsaturated hydraulic conductivity.

Acknowledgment

The study was supported by a special foundation by the *Chinese Academy of Sciences (Grant No. O7R70020SD).*

References

Allen, R. G., Pereira, L. S., Raes, D., Smith, M. (1998): Crop evapotranspiration: Guidelines for computing crop requirements. Irrigation and Drainage Paper No. 56. FAO, Rome, Italy.

Deng, J. C., Chen, X. M., Zhang, J. B., Zhu, A. N. (2002): Saturated hydraulic conductivities of three soil in Huang-Huai-Hai Plain. (In Chinese) *Irrigation and Drainage* 21, 1–4.

Diekkrüger, B., Sondgerath, D., Kersebaum, K. C., McVoy, C. W. (1995): Validity Of Agroecosystem Models – A Comparison Of Results Of Different Models Applied To The Same Data Set. *Ecol. Model.* 81, 3–29.

Eitzinger, J., Stastna, M., Zalud, Z., Dubrovsky, M. (2003): A simulation study of the effect of soil water balance and water stress on winter wheat production under different climate change scenarios. *Agric. Water Manage.* 61, 195–217.

Giakoumakis, S. G., Tsakiris, G. P. (1991): Eliminating the Effect of Temperature from Unsaturated Soil Hydraulic Functions. *J. Hydrol.* 129, 109–125.

Huang, G. H. (2004): Modeling soil water regime and corn yields considering climatic uncertainty. *Plant Soil* 259, 221–229.

Jacques, D., Simunek, J., Timmerman, A., Feyen, J. (2002): Calibration of Richards' and convection-dispersion equations to field-scale water flow and solute transport under rainfall conditions. *J. Hydrol.* 259, 15–31.

Jalota, S. K., Arora, V. K. (2002): Model-based assessment of water balance components under different cropping systems in northwest India. *Agric. Water Manage.* 57, 75–87.

Kendy, E., Gerard-Marchant, P., Walter, M. T., Zhang, Y. Q., Liu, C. M., Steenhuis, T. S. (2003): A soil-water-balance approach to quantify groundwater recharge from irrigated cropland in the North China Plain. *Hydrol. Process.* 17, 2011–2031.

Li, H. M., Inanaga, S., Li, Z. H., Eneji, A. E. (2005): Optimizing irrigation scheduling for winter wheat in the North China Plain. *Agric. Water Manage.* 76, 8–23.

Lin, L. I. (1989): A Concordance Correlation-Coefficient To Evaluate Reproducibility. *Biometrics* 45, 255–268.

Lin, L., Hedayat, A. S., Sinha, B., Yang, M. (2002): Statistical methods in assessing agreement: Models, issues, and tools. *J. Am. Statist. Ass.* 97, 257–270.

Liu, C. M., Zhang, X. Y., Zhang, Y. Q. (2002): Determination of daily evaporation and evapotranspiration of winter wheat and maize by large-scale weighing lysimeter and micro-lysimeter. *Agric. Forest Meteorol.* 111, 109–120.

Liu, S. C., Zhang, Y. P., Zhu, J. C., Ma, A. S. (2000): Effect of temperature on unsaturate soil water movement. (In Chinese) *Acta Univ. Agric. Boreali-occidentalis* 28, 28–33.

Liu, Y., Teixeira, J. L., Zhang, H. J., Pereira, L. S. (1998): Model validation and crop coefficients for irrigation scheduling in the North China plain. *Agric. Water Manage.* 36, 233–246.

Maraux, F., Lafolie, F., Bruckler, L. (1998): Comparison between mechanistic and functional models for estimating soil water balance: deterministic and stochastic approaches. *Agric. Water Manage.* 38, 1–20.

Rana, G., Katerji, N. (2000): Measurement and estimation of actual evapotranspiration in the field under Mediterranean climate: a review. *Eur. J. Agron.* 13, 125–153.

Serrano, S. E. (2004): Modeling infiltration with approximate solutions to Richard's equation. *J. Hydrol. Eng.* 9, 421–432.

Shang, S. H., Li, X. C., Mao, X. M., Lei, Z. D. (2004): Simulation of water dynamics and irrigation scheduling for winter wheat and maize in seasonal frost areas. *Agric. Water Manage.* 68, 117–133.

Tenberge, H. F. M., Metselaar, K., Jansen, M. J. W., Desanagustin, E. M. (1995): The Sawah Riceland Hydrology Model. *Water Resour. Res.* 31, 2721–2732.

Wang, H. X., Zhang, L., Dawes, W. R., Liu, C. M. (2001): Improving water use efficiency of irrigated crops in the North China Plain–measurements and modelling. *Agric. Water Manage.* 48, 151–167.

Wegehenkel, M. (2005): Validation of a soil water balance model using soil water content and pressure head data. *Hydrol. Process.* 19, 1139–1164.

Willmott, C. J. (1981): On the validation of models. *Phys. Geo.* 2, 184–194.

Willmott, C. J. (1984): On the evaluation of model performance in physical geography. Spatial statistics and models. D. Reidel Pub., Co., Boston, MA, pp. 184–194.

Zhang, X. (1999): Crop root growth and distribution in soil in the North China Plain. (in Chinese) Meteorological Press, Beijing.

Zhang, Y. Q., Wegehenkel, M. (2006): Integration of MODIS data into a simple model for the spatial distributed simulation of soil water content and evapotranspiration. *Remote Sens. Environ.* 104, 393–408.

Zhang, Y. Q., Liu, C. M., Yang, Y. H., Shen, Y. J. (2001): Effect of soil water stress on CO_2/H_2O exchange parameters in wheat leaves. (in Chinese) *Chin. J. Ecol.* 20, 8–11.

Zhang, Y. Q., Liu, C. M., Shen, Y. J., Kondoh, A., Tang, C. Y., Tanaka, T., Shimada, J. (2002): Measurement of evapotranspiration in a winter wheat field. *Hydrol. Process.* 16, 2805–2817.

Zhang, Y. Q., Kendy, E., Yu, Q., Liu, C. M., Shen, Y. J., Sun, H. Y. (2004): Effect of soil water deficit on evapotranspiration, crop yield, and water use efficiency in the North China Plain. *Agric. Water Manage.* 64, 107–122.

Zhu, A. N., Zhang, J. B., Zhao, B. Z., Cheng, Z. H., Li, L. P. (2005): Water balance and nitrate leaching losses under intensive crop production with Ochric Aquic Cambosols in North China Plain. *Environ. Int.* 31, 904–912.

